Advanced concepts of electron beam pumped excimer lasers

F. K. Tittel, P. Canarelli, C. B. Dane, Th. Hofmann, R. Sauerbrey, T. E. Sharp, G. Szabó, W. L. Wilson, P. J. Wisoff, and S. Yamaguchi

Department of Electrical and Computer Engineering, Rice University, Houston, TX 77251-1892

ABSTRACT

The development of scalable high power lasers in the UV-visible range and ultrashort high brightness laser sources will have significant impact in a number of key technologies. Experiments of scaling the e-beam pumped $XeF(C \rightarrow A)$ laser system to the 1 Joule/pulse output level at a 1 Hz repetition rate are described. Recent progress in the amplification of tunable ultrashort laser pulses in the visible spectrum, utilizing the broadband $XeF(C \rightarrow A)$ excimer transition, is also reported.

1. SCALING CHARACTERISTICS OF THE $XeF(C \rightarrow A)$ EXCIMER LASER

Excimer lasers play an important role in many specific applications that utilize their unique characteristics such as high average power for material processing, and high spectral purity and broad band tunability for remote sensing, optical communication and basic physics research. There is considerable interest in the $XeF(C \rightarrow A)$ excimer laser as an efficient, tunable source of radiation in the blue-green region of the spectrum. Using an electron beam as an excitation source and a kinetically tailored five component gas mixture,[1] efficient operation of this laser system has been demonstrated for short pulse 10 ns (10 MW/cm^3),[2] intermediate pulse 250 ns (~1 MW/cm^3),[3] and long pulse 700 ns (~250 kW/cm^3)[4] electron beam pumping durations. When the short pulse, high current density electron beam excitation technique is employed, peak values of small signal gain exceed 3% cm^{-1}, permitting efficient injection controlled operation. This results in a very effective method for wavelength tuning. Continuous tuning between 450 and 530 nm with a linewidth as narrow as 0.001 nm and good spatial beam quality (3 x diffraction limit) have been demonstrated. An output energy density of ~1.7 J/ℓ with an intrinsic efficiency of 1.3% has been achieved for wavelengths between 470 and 510 nm.[5]

With its gaseous active medium, the $XeF(C \rightarrow A)$ excimer laser is readily scalable to the high energy and power required for numerous potential applications. Experiments are described here that characterize the successful scaling of an electron beam pumped $XeF(C \rightarrow A)$ laser from an active laser volume of ~0.02 ℓ[6] to one of ~0.5 ℓ with a pumped length of 50 cm. An improved output energy of 1.2 J/pulse in repetitive operation of up to 1 Hz, was achieved with a large aperture square unstable resonator geometry, using a compact, halogen compatible, closed flow loop incorporating a transverse in-line fan for gas circulation.

The electron beam generator, described in detail elsewhere,[2, 7, 8] produces a 650 keV, 90 kA pulse in 10 ns (FWHM) with a current density of 250 A/cm^2. The generator was specifically designed for this application and is capable of repetitive operation at up to 1 Hz. The electron beam enters the laser chamber transversely through a 25 μm titanium foil anode coated with a 5 μm layer of ion vapor deposited aluminum to prevent its interaction with the reactive fluorine in the laser gas mixtures. A 0.2 Tesla magnetic guide field provides a three-fold increase in the electron beam current density that is delivered at the optical axis of the laser chamber.

A cross-sectional schematic of the flow system is depicted in Fig. 1. The cross-sectional inner dimensions of the laser cell were 5 cm in width and 6.5 cm in height. The gas was circulated by a transverse flow fan magnetically coupled to an external induction motor. The dimensions of the flow loop design were, to a large extent, constrained by the electron beam diode and the magnetic coil geometries, since both of these could not be changed without considerable difficulty. The resulting 90 degree bend in the flow channel could form turbulent eddies which would interrupt the exchange of gas and degrade the flow uniformity inside the laser cell even at moderate gas flow velocity. To avoid this, four concentric guide vanes were installed in each bend to minimize turbulence effects inside the laser chamber. Moreover, these bending contour on the top and bottom of the laser cell also provided a gradual expansion and contraction of the flowing gas, since the flow loop must be expanded from 2.2 cm in the flow channel to 5.0 cm in the laser chamber. The outside total dimensions of the closed flow loop were 20, 40 and 70 cm, in height, width and length, respectively. The overall gas volume of this set up was approximately 24 ℓ which is a ~6 times larger volume than that used in the previous laser cell described in references 2 and 7.

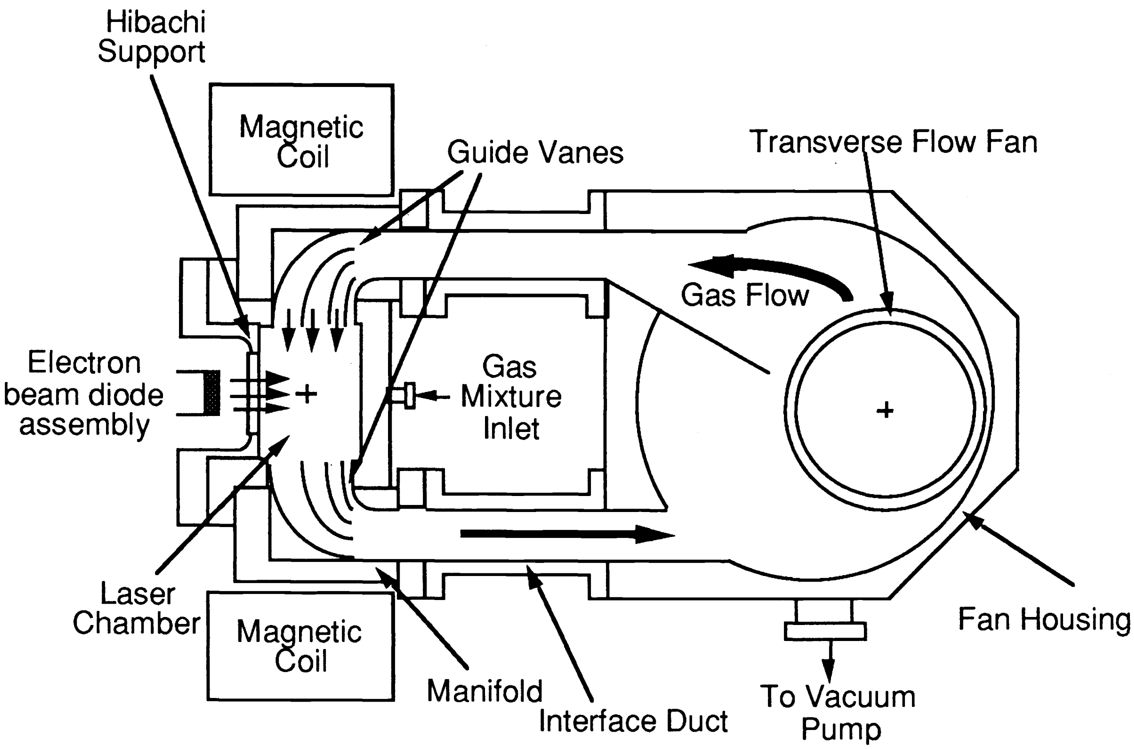

Fig. 1 Cross sectional schematic of the closed flow loop incorporating a transverse in-line fan.

The electron beam energy deposition into the active medium was measured by using chlorostyrene film dosimetry. A cross-sectional contour of the deposition energy at 6.5 bar Ar is shown in Figure 2. The averaged spatial energy density for the cross-section of the resonator volume was measured to be ~110 J/ℓ.[7] To take full advantage of the pumped electron beam volume, a square resonator geometry with an aperture dimension of 4.6 cm x 4.6 cm was designed for maximum laser output energy extraction.

The optical cavities investigated in these experiments were positive branch confocal unstable resonators illustrated schematically in Fig. 3. A resonator magnification of 1.67 was chosen for optimized performance in a mixture consisting of 1.3 mbar F_2, 16 mbar NF_3, 16 mbar Xe, and 1 bar Kr and completed to a total pressure of 6.5 bar with Ar as the buffer.[7] The plano concave total reflector (radius of curvature of 3.0 m) had a highly reflective coating (R>99.9 %) and an AR coating deposited on the concave and the flat surface, respectively. An injection seed laser beam entered the resonator through a 1.5 mm diameter hole in the high reflectivity coating located at the center of this reflector on the concave surface. The output reflector consisted of a double meniscus lens with radii of curvature ±1.8 m and a 2.8 cm x 2.8 cm square reflective coating centered on the convex surface as shown in Fig. 3. These mirrors also had fluorine protective coatings and were mounted directly on the ends of the laser cell in contact with the laser gas mixture spaced 60 cm apart. A *XeCl* excimer laser pumped dye laser provided a 40 ns (FWHM) long injection pulse which resulted in good temporal overlap with the gain duration (~20 ns) in the electron beam pumped amplifier. The seed beam diameter was adjusted with a telescope to achieve uniform injection and the typical peak injection intensity coupled through the hole corresponded to ~3 MW /cm^2. In principal, it is possible to use other more compact external or self injection schemes. One such proposed scheme that is being presently investigated is the use of an appropriately tailored gas mixture to generate both $XeF(B \rightarrow X)$ and $XeF(C \rightarrow A)$ emission and the generation of the second Stokes component of $XeF(B \rightarrow X)$ at 499 nm in H_2, which then can control the $XeF(C \rightarrow A)$ laser output.

The output energy of the injection controlled $XeF(C \rightarrow A)$ amplifier was monitored by a pyroelectric detector, and the temporal pulse duration, typically 10 ns in FWHM, was detected by a fast vacuum photodiode. The spectral characteristics were measured by a 0.25 m spectrometer with an optical multi-channel analyzer(OMA).

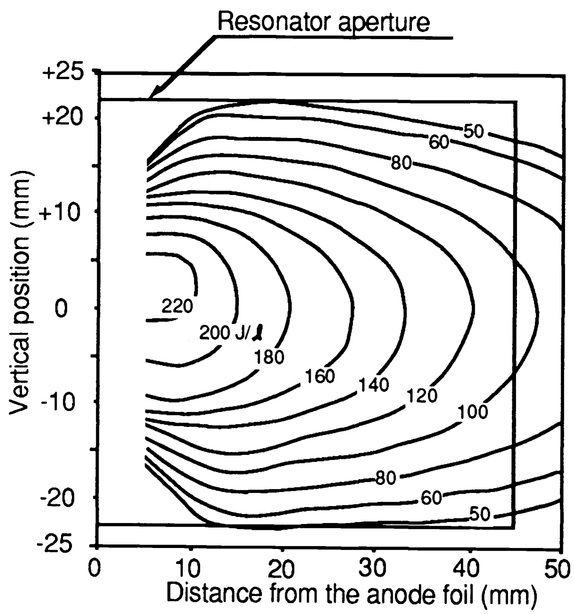

Fig. 2 Energy deposition profile within the e-beam pumped laser chamber experimentally measured by using chlorostyrene film dosimetry.

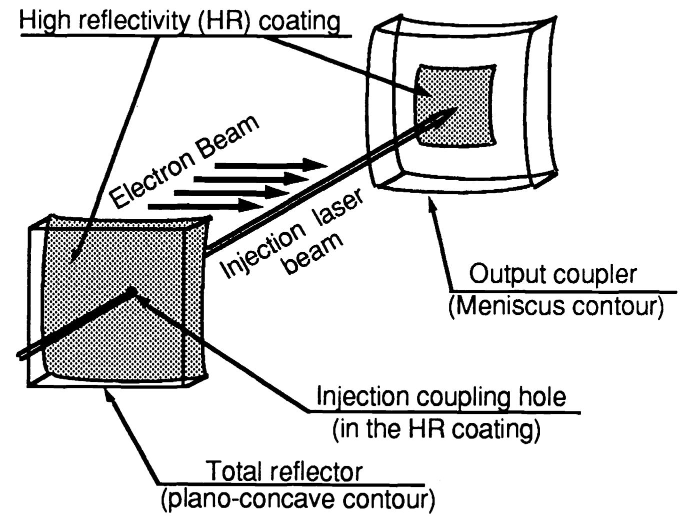

Fig. 3 Schematic drawing of a large aperture unstable resonator configuration.

The time history of flow recovery in the active volume after an electron beam pump pulse was recorded with a Michelson interferometer. The interferometer was illuminated by the excimer pumped dye laser (40 ns, FWHM) tuned to 490 nm. Interferograms were taken at various times during and after electron beam pump pulse deposition into a gas mixture, consisting of 1 bar *Kr* and 5.5 bar *Ar* by adjusting the trigger delay between the electron beam generator and the dye laser. The temporal jitter between the probe pulse and the electron beam firing was less than 10 ns. The sensitivity of the interferometer (per fringe shift) corresponded to a gas density variation ($d\rho/\rho$) of 5×10^{-4} for 6.5 bar *Ar*.[9] The imaging system used to record the interferometric pattern consisted of a two dimensional charge coupled device (CCD) array with 240 x 240 pixels in a 5.5 mm x 6.5 mm distribution with a saturation light level of 1 μJ/cm^2 at the visible wavelengths. The interferometer output was sampled using an uncoated quartz beam splitter and the image was focused onto the CCD array using a 50 cm focal length lens. The attenuation of the image intensity was completed by the neutral density filters located in front of the CCD camera.

The flow velocities were measured to be 5.7 m/s and 5.2 m/s, at the center and at the edge, respectively for 6.5 bar *Ar*, resulting in good uniformity to within 10 % across the flow channel. This flow velocity corresponds to the exchange of approximately 35 laser cell fills between electron beam shots at 1 Hz. Interferograms were taken during and after an electron beam pump pulse to determine the minimum optical cavity recovery time of this device. Initial flow quality without an electron beam shot showed that the gas density variation in the active region of laser chamber was less than the interferometer sensitivity, demonstrating excellent flow uniformity despite the 90 degree bend in the flow loop. Moreover, it was observed that the transient turbulence induced in the laser gas was completely removed 40 ms after the electron beam pulse. Therefore, this compact closed flow loop could achieve stable laser output energy performance at repetition rates of up to 25 Hz.

In single laser shot operation, the timing between the electron beam and injection dye laser was carefully adjusted to obtain optimum laser pulse energy stability. A maximum energy per pulse of 1.2 J was extracted at an injection wavelength of 486.8 nm using the square unstable resonator geometry. Repetitive laser performance was demonstrated in Fig. 4 which depicts the signal from a pyroelectric energy monitor for 10 shots in a 1 Hz sequence. The output energy remained constant throughout the 1 Hz series at the same output level as observed under single shot operation, without shot-to-shot energy degradation due to thermal turbulence. Thus, both the high laser energy output and repetitively pulsed operation were demonstrated for a scaled electron beam pumped *XeF(C→A)* laser amplifier system.

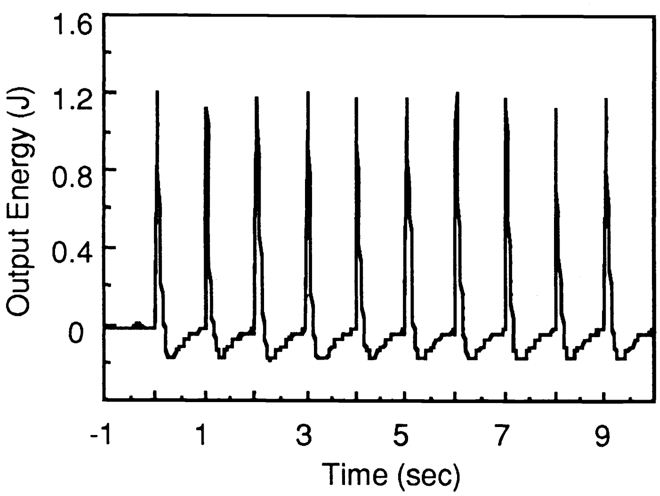

Fig. 4. *XeF(C→A)* laser output energy. The trace depicts 10 individual shots obtained in a 1 Hz sequence. The wavelength and spectral width are 486.8 nm and 0.005 nm, respectively.

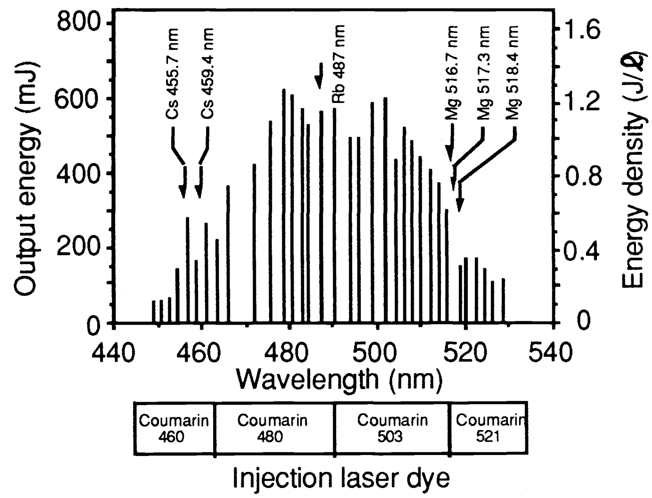

Fig. 5. Wavelength tuning characteristics of the injection controlled *XeF(C→A)* laser.

Shown in Fig. 5 is the output energy of the *XeF(C→A)* injection controlled laser of wavelengths between 450 and 530 nm chosen not to coincide with known narrow band atomic absorbers. The injection dye laser had a linewidth of 0.005 nm, and the data were normalized to an injection intensity of 2 MW/cm^2. A tuning bandwidth of ~50 nm (FWHM), centered at 490 nm, was observed for this injection intensity with a peak specific energy density of 1.3 J/ℓ. A maximum laser output of 0.7 J was measured at 486.8 nm with an intrinsic efficiency of 1.2 %. Even in the wings of the gain profile, at 450 and 530 nm, an energy density of 0.2 J/ℓ was obtained with complete spectral control of the laser output. Also indicated in Fig. 5 are the four injection dyes used to span the *XeF(C→A)* spectral region. The spectral bandwidth of the output of both the injection laser and the *XeF(C→A)* amplified laser output were measured with an air spaced etalon. The spectral bandwidth of the tuned output from the *XeF(C→A)* laser was found to completely preserve that of the injection dye laser for linewidth as narrow as 0.001 nm. As illustrated in Fig. 5, the accessible spectral regions includes the wavelength of various atomic resonance filters. These results make the *XeF(C→A)* laser an attractive candidate for applications requiring high-power, wavelength tunability and spectral bandwidth control such as optical communications.

2. ULTRASHORT LASER PULSE AMPLIFICATION IN THE *XeF(C→A)* GAIN MEDIUM

An ultrashort laser pulse amplifier should have a broad and uniform bandwidth, a high capacity for energy storage and a low level of amplified spontaneous emission (ASE). *XeCl* and *KrF* excimer amplifiers have been extensively studied and utilized as ultrashort laser pulse amplifiers in the ultraviolet.[10-16] These systems, however, have a limited bandwidth (< 5 nm) and large cross-section for stimulated emission that result in low saturation thresholds (E_{sat} ~1-2 mJ/cm^2) and high ASE levels. Other ultrashort laser pulse amplifier media such as dyes or solid state materials are limited in performance by induced nonlinear effects at high intensities. Although this limitation has been largely circumvented by the use of chirped pulse amplification,[17] this technique is still restricted by the bandwidth region over which the chirped pulse can be amplified as well as by the difficulty in scaling the condensed media amplifiers (or compressor components such as gratings) to large apertures. Recently, we reported an alternative approach to amplify subpicosecond laser pulses in an electron beam pumped *XeF(C→A)* excimer amplifier.[18] Figure 6 provides an illustrative comparison of the fluorescence spectrum of the *XeF(C→A)* amplifier along with that of the free-running laser. Assuming the entire spectral bandwidth could be fully used for the amplification, pulses of <10 fs could be amplified. Unlike the *XeCl* and *KrF(B→X)* amplifiers, the *XeF(C→A)* excimer transition has a very broad bandwidth (> 70 nm), and, due to its relatively low gain, exhibits both a high energy saturation threshold and low ASE.

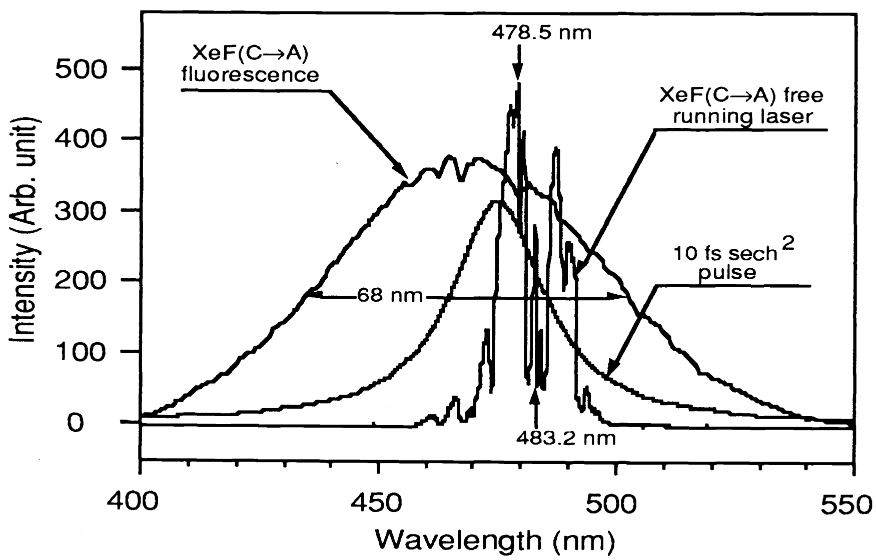

Fig. 6. Time integrated spectra of the *XeF(C→A)* fluorescence and laser. The absorption lines in the free running laser spectrum are due to transient atomic species induced by the electron beam excitation. Also the spectrum of a 10 fs sech^2 pulse is compared with these spectra.

For ultrashort pulse injection experiments, a broadly tunable blue-green dye laser system in the subpicosecond time regime was constructed, as shown in Fig. 7.[19] This system consists of a hybrid synchronously pumped dye oscillator with the output amplified in a two-stage dye amplifier. The oscillator is pumped with the third harmonic of a cw mode-locked Nd:YAG laser, and the dye amplifiers are pumped with the third harmonic of the regeneratively amplified Nd:YAG laser output. The new two-stage dye amplifier design[19] produced tunable ~ 2 mJ, 850 fs laser pulses with an ASE content of less than 0.1% for injection into the *XeF(C→A)* amplifier.

The temporal peak of the measured single pass gain of the *XeF(C→A)* amplifier at 478.5 nm, subsequent to electron beam excitation, is depicted in Figure 8. The 478.5 nm wavelength corresponds to a peak in the output of the free-running spectrum of the *XeF(C→A)* laser as shown in Figure 6. The gain was measured with two calibrated vacuum photodiodes and carefully calibrated beam splitters and neutral density filters. The peak small signal gain was 3.5 % cm^{-1}, which is comparable to the peak small-signal gains measured in earlier nanosecond pulse probe experiments.[7] Reduction in the gain due to polarization of the probe beam was not observed. This is consistent with the duration of the probe pulses being on the order of the rotational reorientation time, which is estimated to be 0.8 ps by using the 0.28 nm internuclear distance of the *XeF(B)* state.[20] In addition, as shown in Fig. 8, the gain was greater than 3% cm^{-1} for more than 10 ns, allowing future multipass experiments to optimize energy extraction from an electron beam pumped *XeF(C→A)* amplifier.

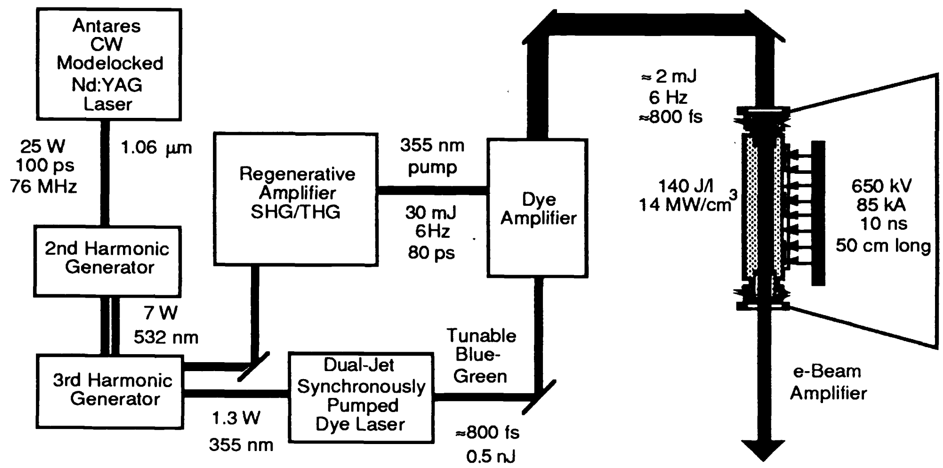

Fig. 7 Diagram of a subpicosecond *XeF(C→A)* laser amplifier system.

Figure 9 shows a plot of the single pass gain as a function of the input energy density at 478.5 nm. The solid line represents a Frantz-Nodvik curve[21] corresponding to a saturation energy of 120 mJ/cm^2. Since the absorption cross-section of the identified saturable absorbers is typically three to four orders of magnitude larger than the stimulated emission cross-section of the *XeF(C→A)* transition,[22] the saturable absorbers are expected to be fully saturated at injection energies below the energy scale of Fig. 9. Therefore, we believe that the Frantz-Nodvik line provides at least a qualitative description of the gain saturation even though the model generally does not allow for the presence of saturable absorbers. Since the questions related to the applicability of the Frantz-Nodvik model could be fully resolved only on the basis of a better knowledge of the saturable absorbers involved, values for the saturation energy are necessarily ambiguous. The experiments, however, have clearly demonstrated that output energy densities as high as 170 mJ/cm^2 can be achieved with the *XeF(C→A)* amplifier. In order to fully utilize the broad emision band of the *XeF(C→A)* amplifier to amplify short pulses, the absorption valleys in the free-running spectrum must saturate at high injection intensities, providing the same gain over the entire spectral region. Data taken at 483.2 nm which corresponds to a valley in the output of the free-running spectrum of the *XeF(C→A)* laser show a single-pass gain at an injection intensity of 25 mJ/cm^2 equivalent to the single-pass gain at 478.5 nm. The ASE content of the *XeF(C→A)* amplifier output was less than 0.001%.

In an attempt to achieve higher output energy densities by double-passing the gain region, spatial beam confinement appeared. Figure 10 depicts the evolution of the amplified beam profile, as measured with a CCD beam imaging system, for one and two passes through the *XeF(C→A)* amplifier. The spike that appears in the double-passed pulse contained ~ 6% of the pulse energy and was 10 times narrower than the initial injection pulse. It was found that the spatial narrowing occurred at about two times lower input energy densities when operating in a valley of the free running *XeF(C→A)* laser as opposed to a peak, suggesting that the effect may be related to the presence of saturable absorbers. In addition, the spatial narrowing appeared to occur in the gas medium rather than in the optics of the system. The 0.5 inch thick fused silica windows were removed from the gas cell and exposed to high energy densities from the dye amplifier to check for self focussing. At energy densities of up to 4 J/cm^2, no beam narrowing was observed; however, the windows did show self-induced absorption effects at high intensities. Since the intensity for the gain measurements was always below ~200 mJ/cm^2, the window absorption was not important for the measurements presented here.

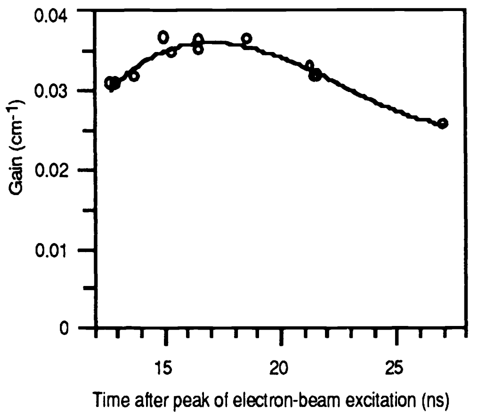

Fig. 8 Temporal evolution of the $XeF(C\rightarrow A)$ gain at 478.5 nm after electron-beam excitation. The pulse duration of the probe beam is 500 fs, the energy flux is 20 mJ/cm^2.

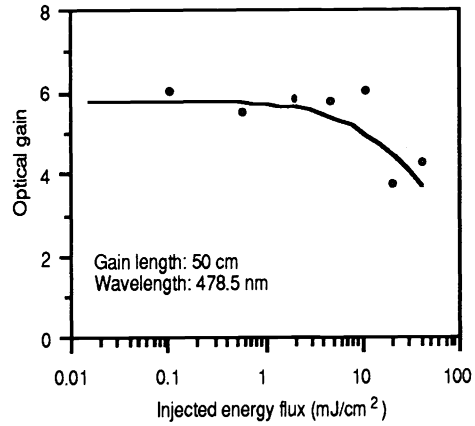

Fig. 9 Single pass gain as a function of output energy density.

The temporal shape of the ultrashort pulses was not significantly affected during amplification. Figure 11 shows a single-shot autocorrelation of an amplified pulse at 478.5 nm with an output energy density of about 40 mJ/cm^2. The autocorrelator used in this experiment was similar to the one described in reference 23. The solid line represents a calculated fit assuming an asymmetric exponential (1:5 rise/fall ratio) pulse shape with an 800 fs pulse duration. Further work in compression of the probe pulse should yield pulse durations sufficiently short to allow for measurement of the XeF rotational reorientation time and permit more detailed studies of the spectral uniformity of the gain.[19]

The saturation energy density of the $XeF(C\rightarrow A)$ amplifier represents about 50 times improvement in energy storage over $XeCl$ and KrF amplifiers. In addition, the bandwidth of the $XeF(C\rightarrow A)$ transition of ~70 nm may be sufficient to amplify pulses of considerably shorter duration, such as the recently reported 10 fs blue-green pulse produced by white-light continuum filtering.[24]

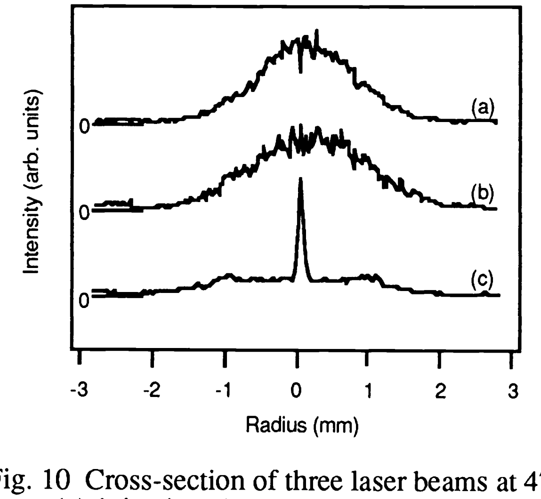

Fig. 10 Cross-section of three laser beams at 478.5 nm: (a) injection dye laser, energy 0.75 mJ, (b) beam after 50 cm gain length, energy 2.9 mJ, and (c) beam after 100 cm gain length, energy 3.2 mJ. The relative intensity of each curve was adjusted to fit the plotting area.

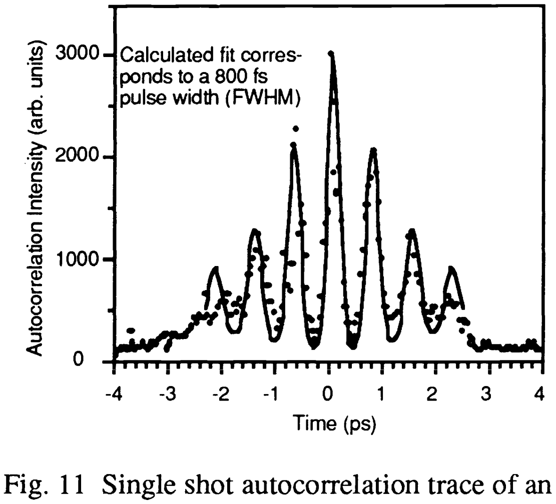

Fig. 11 Single shot autocorrelation trace of an amplified pulse at 478.5 nm. The calculated fit assumes an asymmetric pulse shape with an 800 fs pulse duration

3. SUMMARY

Scaling experiments of an injection controlled *XeF(C→A)* laser pumped by an intense short pulse electron beam have been performed. Using a multi-component high pressure gas mixture comprised of F_2, NF_3, *Xe*, *Kr*, and *Ar*, a specific laser energy output density of 1.7 J/ℓ with an intrinsic efficiency of 1.3 % were achieved at 486.8 nm, corresponding to an output energy of 0.8 J. Furthermore, the short pulse electron beam excited *XeF(C→A)* excimer laser was demonstrated to be continuously tunable between 450 nm and 530 nm with an output linewidth as narrow as 0.001 nm. Improved laser performance of 1.2 J per pulse and, in particular, repetitive operation of up to 1 Hz using a compact, gas flow (~5.7 m/s) system has been achieved.

In addition, the broad gain bandwidth, which is significantly larger than those available from organic dyes and UV excimer lasers, makes the *XeF(C→A)* system a suitable medium for the amplification of ultrashort laser pulses to the terawatt level in the blue green. The feasibility of developing an ultrahigh brightness laser source in the visible based on the *XeF(C→A)* transition has been established.

4. ACKNOWLEDGEMENTS

The authors would like to thank Jim Hooten at Rice University for his technical assistance. Helpful comments by W. L. Nighan of United Technologies Research Center (UTRC) are sincerely appreciated. This work was supported by the Office of Naval Research, Air-Force Office of Scientific Research, and the Robert Welch Foundation.

5. REFERENCES

1. W. L. Nighan, R. Sauerbrey, Y. Zhu, F. K. Tittel, and W. L. Wilson, "Kinetically tailored properties of electron beam excited *XeF(C→A)* and *XeF(B→X)* laser media using an *Ar-Kr* buffer mixture", *IEEE J. Quantum Electron.* vol. QE-23, pp. 253-261, 1987. and W. L. Nighan, and M. C. Fowler, "Kinetic processes in electron beam-excited *XeF(C→A)* laser media", *IEEE J. Quantum Electron.* vol. QE-25, pp. 791-802, 1989.

2. G. J. Hirst, C. B. Dane, W. L. Wilson, R. A. Sauerbrey, F. K. Tittel, and W. L. Nighan, "Scaling of an injection-controlled *XeF(C→A)* laser pumped by a repetitively pulsed, high current density electron beam," *Appl. Phys. Lett.*, 54 (19), pp1851-1853, 1989.

3. P. J. M. Peters, H. M. J. Bastiaens, W. J. Witteman, R. Sauerbrey, C. B. Dane, and F. K. Tittel, "Efficient *XeF(C→A)* laser excited by a coaxial e-beam at intermediate pumping rates", submitted to *IEEE J. Quantum Electron.*

4. A. Mandl and L. N. Litzenberger, "Efficient, long-pulse *XeF(C→A)* laser at moderate electron beam pumping rate," *Appl. Phys. Lett.* 53 (18), 1690-1692, 1988. and L. N. Litzenberger and A. Mandl "Improvements in long pulse, electron beam pumped *XeF(C→A)* laser performance," *Proc. of SPIE*, SPIE vol. 1225, pp. 60-85, 1990.

5. C. B. Dane, S. Yamaguchi, Th. Hofmann, R. Sauerbrey, W. L. Wilson, and F. K. Tittel, "Spectral characteristics of an injection controlled *XeF(C→A)* excimer laser," *Appl. Phys. Lett.* vol. 56, pp. 2604-2606, 1990.

6. N. Hamada, R. Sauerbrey, W. L. Wilson, F. K. Tittel, and W. L. Nighan "Performance characteristics of an injection-controlled electron-beam pumped *XeF(C→A)* laser system," *IEEE J. Quantum Electron.*, vol. QE-24, pp. 1571-1578, 1986.

7. C. B. Dane, G. J. Hirst, S. Yamaguchi, Th. Hofmann, W. L. Wilson, R. A. Sauerbrey, F. K. Tittel, W. L. Nighan, and M. C. Fowler, "Scaling characteristics of the *XeF(C→A)* excimer laser," to be published in *IEEE J.Quantum Electron.*, Special Issue on Electronic Transition Gas Lasers, September, 1990.

8. S. Lloyd, Y. G. Chen, G. McAllister, M. Montgomery, T. Olson, J. Shannon, B. Dane, G. Hirst, R. Sauerbrey, F. Tittel, and W. Wilson, "A 500kV rep-rate electron beam generator," *Proceedings of the Seventh IEEE Pulsed Power Conference*, Monterey CA,1989.

9. R. J. Goldstein, "Optical systems for flow measurement: shadowgraph, schlieren, and interferometric techniques", in *Fluid Mechanics Measurements*, Washington: Hemisphere, 1983.

10. P.B. Corkum and R. S. Taylor, "Picosecond amplification and kinetic studies of *XeCl*", *IEEE J. Quantum Electron.*, vol. QE-18, pp. 1962-1975, 1982.

11. S. Szatmári, B. Rácz, and F. P. Schäfer, "Bandwidth limited amplification of 220 fs pulses in *XeCl*", *Opt. Commun.*, vol. 62, pp. 271-276, 1987.

12. S. Szatmári, and F. P. Schäfer, " Comparative study of the gain dynamics of *XeCl* and *KrF* with subpicosecond resolution", *J. Opt. Soc. Am. B*, vol. 4, pp. 1943-1948, 1987.

13. J. H. Glownia, G. Arjavalingan, P. P. Sorokin, and J. E. Rothenberg, "Amplification of 350-fsec pulses in *XeCl* excimer gain modules", *Opt. Lett.*, vol. 11, pp. 79-81, 1986.

14. A. J. Taylor, T. R. Gosnell, and J. P. Roberts, "Ultrashort-pulse energy-extraction measurements in *XeCl* amplifiers", *Opt. Lett*, vol. 15, pp. 118-120, 1990.

15. S. Watanabe, A. Endoh, M. Watanabe, N. Sarukura, and K. Hata, "Multiterawatt excimer-laser system", *J. Opt. Soc. Am.B*, vol. 6, pp. 1870-1876, 1989.

16. A. P. Schwarzenbach, T. S. Luk, I. A. McIntyre, U. Johann, A. McPherson, K. Boyer, and C. K. Rhodes, "Subpicosecond *KrF** excimer laser source", *Opt. Lett.*, vol. 11, pp. 499-501, 1986.

17. P. Maine, D. Strickland, P. Bado, M. Pessot, and G. Mourou, "Generation of ultrahigh peak power pulses by chirped pulse amplification", *IEEE J. Quantum Electron.*, vol. QE-24, pp. 398-403, 1988.

18. T. E. Sharp, Th. Hofmann, C. B. Dane, W. L. Wilson, F. K. Tittel, P. J. Wisoff, and G. Szabó, "Ultrashort laser pulse amplification in a $XeF(C \rightarrow A)$ excimer amplifier", submitted to *Optics Lettes*.

19 T. E. Sharp, C. B. Dane, F. K. Tittel, P. J. Wisoff, and G. Szabó, "A tunable, high power, subpicosecond blue-green dye laser system with a two stage dye amplifier design", submitted to *IEEE J. Quantum Electron.*

20. A. L. Smith, and P. C. Kobrinsky, " Flash photolysis absorption spectroscopy of Xenon Fluoride: vibrational analysis of the B-X transisiton", *J. Molecular Spectroscopy*, vol. 69, pp. 1-10, 1978.

21. L. M. Frantz and J. S. Nodvik, "Theory of pulse propagation in a laser amplifier", *J. Appl. Phys.* , vol. 34, pp. 2346-2349, 1963.

22. N. Hamada, "Studies of an injection controlled rare gas halide excimer laser", PhD Thesis, Rice University, Houston Texas , 1988.

23. G. Szabó, Z. Bor, and A. Muller, "Phase-sensitive single-pulse autocorrelator for ultrashort laser pulses",*Opt. Lett..*, vol. 13, pp. 746 -748, 1988.

24. R. W. Schoenlein, J. Y. Bigot, M. T. Portella, and C. V. Shank, "Generation of blue-green 10 fs pulses using an excimer pumped dye amplifier", *Conf. on Lasers and Electro-Optics*, Anaheim, 1990, postdeadline paper CPDP7.